Available online at www.sciencedirect.com
SCIENCE DIRECT®

Journal of Power Sources 157 (2006) 395–400

JOURNAL OF POWER SOURCES

www.elsevier.com/locate/jpowsour

Short communication

Optimization of a fuel-cell manifold

Yongjin Sung *

Hyundai Motor Company, Fuel Cell System Development Team, 772-1 Jangduk-dong, Whasung-si, Kyunggi-do, 445-706 Republic of Korea

Received 9 May 2005; accepted 29 July 2005
Available online 21 September 2005

Abstract

A design of fuel-cell manifold to evenly distribute the reactants among the channels within bipolar plates is presented. Neglecting the friction term from the momentum equation, one-dimensional governing equations are manipulated to develop the manifold equation to achieve the required design. Some manifold shapes that satisfy the manifold equation, are suggested, together with the distribution of static pressure within the manifold itself.

Keywords: Fuel-cell; Manifold; Design; Optimization

1. Introduction

A fuel-cell stack has a hydraulic network to distribute the reactants among the component cells. The interface between the external source of reactants and the cell inlet and that between the cell outlet and the exhaust plumbing are each known generically as the fuel-cell manifold or header. Two typical configurations of the fuel-cell manifold, e.g., Z-type and U-type, that provide different flow directions are shown in Fig. 1. The research to date has focused on developing the channel distribution for a given manifold design of rectangular cross-section. This study reported here shows how to change the manifold shape to achieve an even distribution of reactants among the channels.

2. Mathematical model

2.1. Z-type

Maharudrayya et al. [1] have proposed an analytical solution for manifold flow with a uniform cross-section. In the work presented here, the manifold is allowed to change its cross-section so as to achieve even distribution among the channels. A schematic diagram of the proposed system and its key dimensions are given in Fig. 2. The upper manifold provides the reactants while the lower manifold collects them after they have passed through the channels. The governing equations for the manifold flow, including the area change, can be written as follows:

Upper manifold

$$\frac{\mathrm{d}(bh_1V_1)}{\mathrm{d}x_1} = -\frac{N}{L}A_\mathrm{c}V_\mathrm{c} \tag{1}$$

$$\frac{\mathrm{d}(\rho bh_1V_1^2)}{\mathrm{d}x_1} = -\frac{\mathrm{d}(P_1bh_1)}{\mathrm{d}x_1} - f\rho V_1^2(b+h_1) \tag{2}$$

Lower manifold

$$\frac{\mathrm{d}(bh_2V_2)}{\mathrm{d}x_2} = \frac{N}{L}A_\mathrm{c}V_\mathrm{c} \tag{3}$$

$$\frac{\mathrm{d}(\rho bh_2V_2^2)}{\mathrm{d}x_2} = -\frac{\mathrm{d}(P_2bh_2)}{\mathrm{d}x_2} - f\rho V_2^2(b+h_2) \tag{4}$$

For convenience, the inlet of the upper manifold is aligned with the first channel and the outlet of the lower manifold with the last channel. The consumption of mass by the electrochemical reaction is assumed not to affect the channel flow. The pressure gradient and flow velocity is given by:

$$P_1 - P_2 \equiv \Delta P_{12} = H\frac{1}{2}\rho V_\mathrm{c}^2, \quad \text{where } H = \frac{4fL_\mathrm{c}}{D_\mathrm{c}} \tag{5}$$

* Tel.: +82 16 729 6849; fax: +82 31 368 6787.
E-mail address: heyman@hyundai-motor.com.

0378-7753/$ – see front matter © 2005 Elsevier B.V. All rights reserved.
doi:10.1016/j.jpowsour.2005.07.067

Nomenclature

A	cross-sectional area
b	manifold width
D	hydraulic diameter
f	friction factor
h	manifold height
H	loss coefficient
L	manifold length
M	flow parameter defined in Eqs. (8) and (9)
N	number of channels
P	static pressure
q	flow rate per unit width of manifold
Re	Reynolds number
V	velocity magnitude
W	channel width
x	co-ordinate along the manifold

Greek letters

α	manifold height ratio
β	manifold height ratio
γ	manifold height ratio
Δ	difference operator
Θ	non-dimensionalized channel pressure drop
μ	viscosity
Π	non-dimensionalized dynamic pressure
ρ	density
Ω	channel pressure drop

Subscripts

1	upper manifold
2	lower manifold
c	channel

$$V_c = \Delta P_{12}\frac{D_c^2}{2\mu L_c(Ref)_c}, \quad \text{where } (Ref)_c = 13.84 + 10.38\,\exp\left(-\frac{3.4b_c}{W_c}\right) \tag{6}$$

The pressure gradient is established within each manifold due to the inertia change and the friction with the wall. The inertia and the friction term can be compared in terms of order of magnitude by:

$$\frac{\text{friction term}}{\text{inertia term}} \sim \frac{f\rho V^2(b+h)}{\Delta(\rho bhV^2)/\Delta x} = O\left(\frac{2fL}{D_h}\right) \tag{7}$$

Since the friction factor for turbulent tube flow is below 0.01, the friction term becomes non-negligible if the hydraulic diameter of the manifold is reduced to below 2% of its length. In this study, the manifold is assumed to have a cross-section of moderate size so as to cause negligible friction. With the introduction of this assumption, the momentum equation can be simplified to:

Upper manifold:

$$\rho\frac{q_1^2}{h_1} + P_1h_1 = \text{const} \equiv M_1 \tag{8}$$

Lower manifold:

$$\rho\frac{q_2^2}{h_2} + P_2h_2 = \text{const} \equiv M_2 \tag{9}$$

To facilitate the manipulation, the main variable was changed from the velocity to the flow rate per unit width, q. Eqs. (8) and (9) are used to calculate the driving force at the channel or the

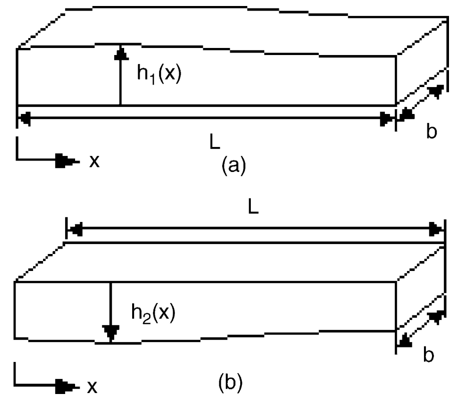

Fig. 2. Schematic diagram of manifold shape with key dimensions: (a) upper manifold; (b) lower manifold.

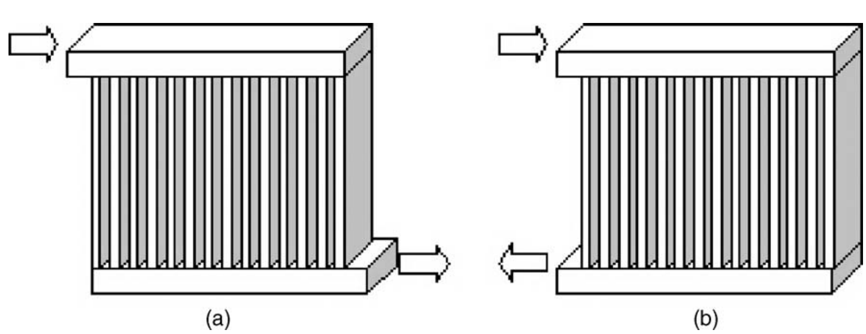

Fig. 1. Fuel-cell manifold: (a) Z-type; (b) U-type.

pressure difference between the upper and lower manifolds:

$$\Delta P_{12} = \frac{M_1}{h_1} - \frac{M_2}{h_2} - \rho\left(\frac{q_1^2}{h_1^2} - \frac{q_2^2}{h_2^2}\right) \tag{10}$$

The continuity equations at both manifolds give rise to the following expression that greatly simplifies the calculation:

$$q_1 + q_2 = \text{const} \equiv q \tag{11}$$

The flow rate q has the value of q_1 at the inlet of the upper manifold or at $x=0$ since q_2 is zero there. Using Eqs. (6) and (10), Eq. (1) can be written in terms of a single unknown variable q_1 if M_1 and M_2 are known, i.e.:

$$\frac{dq_1}{dx} = -\frac{N}{bL}\frac{D_c^2 A_c}{2\mu L_c (Ref)_c} \times \left[\frac{M_1}{h_1} - \frac{M_2}{h_2} - \rho\left(\frac{q_1^2}{h_1^2} - \frac{(q-q_1)^2}{h_2^2}\right)\right] \tag{12}$$

It is worthwhile nothing that q_1 and P_1 are not given simultaneously as input for the simulation. Hence, instead of using Eq. (8) directly to determine M_1, it has been decided to employ the pressure difference at the end of the upper manifold (or at $x=L$) and the reference pressure at the lower manifold, i.e.:

$$M_1 = h_{1,x=L}(P_{\text{amb}} + (\Delta P_{12})_{x=L}) \tag{13}$$

Since the pressure difference is usually available after the calculation, the final solution is obtained after the iteration. M_2 can be calculated from q_2 and P_2 at the outlet of the lower manifold where these two parameters are the flow rate at the inlet of the upper manifold and the ambient pressure, respectively:

$$M_2 = \rho\frac{q^2}{h_{2,x=L}} + P_{\text{amb}} h_{2,x=L} \tag{14}$$

2.2. U-type manifold

A similar formulation to that above is possible for the U-type configuration, it is necessary only to make a slight modification due to the flow direction at the lower manifold. For convenience, the inlet and the outlet are aligned with the first channel from the left in Fig. 1.

Upper manifold:

$$\frac{dq_1}{dx_1} = -\frac{N}{bL} A_c V_c \tag{15}$$

$$\rho\frac{q_1^2}{h_1} + P_1 h_1 = \text{const} \equiv M_1 \tag{16}$$

Lower manifold:

$$\frac{dq_2}{dx_2} = -\frac{N}{bL} A_c V_c \tag{17}$$

$$\rho\frac{q_2^2}{h_2} + P_2 h_2 = \text{const} \equiv M_2 \tag{18}$$

Since the momentum equation does not change, Eq. (10) can still be used to represent the pressure difference between two manifolds of U-type configuration. The continuity equation produces a different relationship between the q_1 and q_2 flow rates, i.e.:

$$q_1 = q_2 \equiv \tilde{q} \tag{19}$$

Using Eqs. (6) and (10), Eq. (15) can be written in terms of single unknown variable $\tilde{q}$ when M_1 and M_2 are known, i.e.:

$$\frac{d\tilde{q}}{dx} = -\frac{N}{bL}\frac{D_c^2 A_c}{2\mu L_c (Ref)_c}\left[\frac{M_1}{h_1} - \frac{M_2}{h_2} - \rho\tilde{q}^2\left(\frac{1}{h_1^2} - \frac{1}{h_2^2}\right)\right] \tag{20}$$

M_1 and M_2 are calculated in different way from Eqs. (13) and (14), since in the outlet of the lower manifold the static pressure is now located at $x=0$. Thus:

$$M_1 = \rho\frac{q^2}{h_{1,x=0}} + h_{1,x=0}(P_{\text{amb}} + (\Delta P_{12})_{x=0}) \tag{21}$$

$$M_2 = \rho\frac{q^2}{h_{2,x=0}} + h_{2,x=0} P_{\text{amb}} \tag{22}$$

3. Optimization of manifold shape

A main goal in the design of a manifold is to distribute the reactants among the channels as even as possible with a moderate size of manifold. As the manifold size increases, it will certainly improve the distribution but will become useless from a practical point of view. By contrast, if its size becomes too small, the pressure drop will be raised and the system will require an uneconomical air blower for the distribution of reactants among the channels. In this section, the manifold shape is optimized to achieve the best compromise in size.

If the manifold is designed to distribute the same amount of reactant among each channel, then the channel velocity and the flow rate through the manifold can be written as:

$$V_c = \frac{qb}{NA_c}, \qquad q_1 = q\left(1 - \frac{x}{L}\right) \tag{23}$$

Using Eq. (6), the pressure drop in the channel is determined without iteration as:

$$\Delta P_{12} = \frac{2\mu L_c (Ref)_c}{D_c^2}\frac{qb}{NA_c} \equiv \Omega \tag{24}$$

3.1. Z-type configuration

Substituting Eq. (23) for q_1 in Eq. (12) yields:

$$\frac{M_1}{h_1} - \frac{M_2}{h_2} - \rho q^2\left(\frac{(1-\bar{x})^2}{h_1^2} - \frac{\bar{x}^2}{h_2^2}\right) = \Omega, \quad \text{where } \bar{x} = \frac{x}{L} \tag{25}$$

The manifold length L was used to normalize the stream-wise co-ordinate. Rearrangement of the terms after substitution of M_1

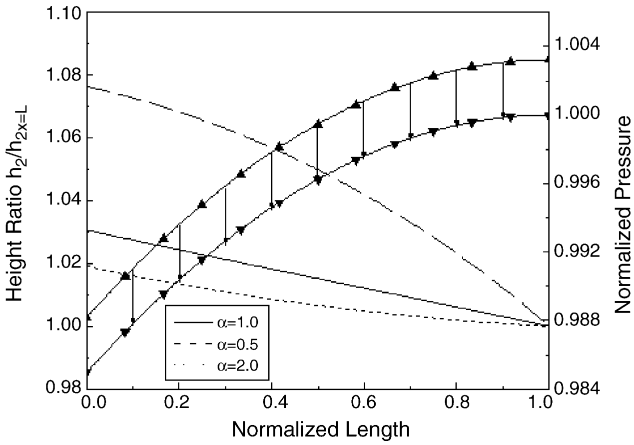

Fig. 3. Profile of lower manifold for $h_1(x)$ = const and normalized static pressure at upper manifold (Z-type).

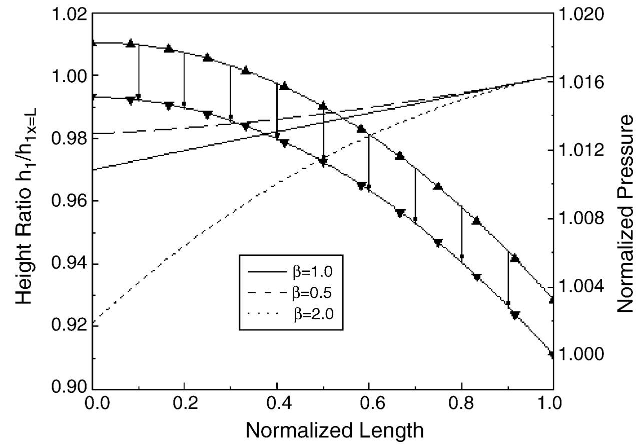

Fig. 4. Profile of upper manifold for $h_2(x)$ = const and normalized static pressure at upper manifold (Z-type).

and M_2 in Eqs. (13) and (14) using Eq. (24) gives:

$$\frac{h_{1,\bar{x}=1}}{h_1}(\Omega + P_{\text{amb}}) - \frac{h_{2,\bar{x}=1}}{h_2}\left(\rho\frac{q^2}{h_{2,\bar{x}=1}^2} + P_{\text{amb}}\right) - \rho q^2\left(\frac{(1-\bar{x})^2}{h_1^2} - \frac{\bar{x}^2}{h_2^2}\right) = \Omega \qquad (26)$$

The various combinations of h_1 and h_2 that satisfy Eq. (26) will render an even distribution among the channels. From the definition of M_1, the static pressure at the upper manifold becomes:

$$P_1 = \frac{h_{1,\bar{x}=1}}{h_1}(P_{\text{amb}} + \Omega) - \rho\frac{q^2}{h_1^2}(1-\bar{x})^2 \qquad (27)$$

3.1.1. $h_1(x)$ = const

To find the specific design that satisfies Eq. (26), the special case is assumed in which the height of the upper manifold is maintained at a constant value. Then:

$$h_{2,\bar{x}=1} = \alpha h_1, \qquad \frac{\rho q^2}{P_{\text{amb}} h_{2,\bar{x}=1}^2} \equiv \Pi,$$

$$\frac{\Omega}{P_{\text{amb}}} \equiv \Theta, \qquad \frac{h_2}{h_{2,\bar{x}=1}} \equiv \bar{h}_2,$$

$$(1 - \alpha^2\Pi(1-\bar{x})^2)\bar{h}_2^2 - (\Pi + 1)\bar{h}_2 + \Pi\bar{x}^2 = 0 \qquad (28)$$

During the derivation of Eq. (28), three scaling variables are suggested: (i) α is the ratio between the heights of both manifolds based on the height at the exit of the lower manifold; (ii) Π is the ratio of dynamic pressure to static pressure at the outlet of the lower manifold; (iii) Θ is the pressure drop in the channel normalized with respect to ambient pressure.

The static pressure at the upper manifold, normalized to ambient pressure, is:

$$\bar{P}_1 = 1 + \Theta - \alpha^2\Pi(1-\bar{x})^2 \qquad (29)$$

The height profile and the static pressure for various α values are plotted in Fig. 3 with h_1 fixed. The static pressure increases along the manifold co-ordinate x to maintain force balance with the reduced inertia. The size of the arrow drawn downward between two curves, i.e., the channel pressure drop (Ω), is shown to be constant along the manifold co-ordinate x. To achieve even distribution for the upper manifold with a uniform cross-section, the lower manifold was modified to have its cross-sectional area decreasing along the co-ordinate. If α decreases or the size of the lower manifold is reduced, the required variation in shape becomes large in order to provide an even distribution. If the number of channels or their area is changed, the scaling variables can be used to rescale the manifold.

3.1.2. $h_2(x)$ = const

In this case, the lower manifold has a uniform area while the upper manifold is allowed to change its cross-section to enable the channel distribution to be even, i.e.:

$$h_{1,\bar{x}=1} = \frac{h_2}{\beta}, \qquad \frac{\rho q^2}{P_{\text{amb}} h_2^2} \equiv \Pi,$$

$$\frac{\Omega}{P_{\text{amb}}} \equiv \Theta, \qquad \frac{h_1}{h_{1,\bar{x}=1}} \equiv \bar{h}_1,$$

$$(1 + \Theta + \Pi(1-\bar{x}^2))\bar{h}_1^2 - (1+\Theta)\bar{h}_1 + \beta^2\Pi(1-\bar{x})^2 = 0 \qquad (30)$$

In this relationship, the scaling variables are defined as: (i) β is the ratio between the heights of both manifolds based on the height at the inlet of the upper manifold; (ii) Π and Θ have the same physical meaning as in Section 3.1.1, but with a different length scale. The normalized static pressure at the upper manifold is:

$$\bar{P}_1 = \frac{1}{\bar{h}_1}(1+\Theta) - \frac{1}{\bar{h}_1^2}\beta^2\Pi(1-\bar{x})^2 = 1 + \Theta + \Pi(1-\bar{x}^2) \qquad (31)$$

The static pressure decreases along the manifold co-ordinate x, as shown in Fig. 4. This may be attributed to the fact that the upper manifold is designed to have the cross-section increasing along the x co-ordinate and the exit of the lower manifold is located at $x = L$. As will be shown later, the shape of manifold exerts less influence on the distribution of static pressure in a U-type configuration where the exit is located in the same co-ordinate with the inlet at $x=0$. The shape of the upper manifold is consistent with that of the lower manifold in Section 3.1.1 because of the symmetry.

3.1.3. $h_1(x) = h_2(L-x)$

A symmetrical manifold design $h_1(x)=h_2(L-x)$ is an obvious consideration given the location of the inlet and the outlet. Introducing the new co-ordinate $\bar{x}' = 1-\bar{x}$ and using the relations $h_1(\bar{x}') = h_2(1-\bar{x}')$ and $h_2(\bar{x}') = h_1(1-\bar{x}')$, Eq. (26) can be rewritten after dropping the prime notation as:

$$\frac{h_{1,\bar{x}=1}}{h_2(\bar{x})}(\Omega + P_{\text{amb}}) - \frac{h_{2,\bar{x}=1}}{h_1(\bar{x})}\left(\rho\frac{q^2}{h_{2,\bar{x}=1}^2} + P_{\text{amb}}\right) - \rho q^2\left(\frac{\bar{x}^2}{h_2(\bar{x})^2} - \frac{(1-\bar{x})^2}{h_1(\bar{x})^2}\right) = \Omega \quad (32)$$

Eq. (26) and (32) are added to produce:

$$\frac{h_{1,\bar{x}=1}}{h_{1,\bar{x}=0}} \equiv \gamma, \qquad \frac{\rho q^2}{P_{\text{amb}} h_{1,\bar{x}=0}^2} \equiv \Pi, \qquad \frac{\Omega}{P_{\text{amb}}} \equiv \Theta,$$

$$\frac{h_1}{h_{1,\bar{x}=0}} \equiv \bar{h}_1, \qquad \frac{1}{\bar{h}_1(\bar{x})} + \frac{1}{\bar{h}_1(1-\bar{x})} = \frac{\gamma+1}{\gamma},$$

$$\text{where } \gamma = \frac{\Theta + \Pi + \sqrt{(\Theta+\Pi)^2 + 4(\Theta+1)(\Pi+1)}}{2(\Theta+1)} \quad (33)$$

Eq. (33) provides many choices in the design of the manifold shape with simpler form than Eq. (26). A profile such as $\bar{h}_1(\bar{x}) = (A\bar{x}+B)^{-1}$ can be used with the coefficients being determined by the substitution to produce:

$$\bar{h}_1(\bar{x}) = \frac{\gamma}{(1-\gamma)\bar{x} + \gamma} \quad (34)$$

The normalized static pressure at the upper manifold is:

$$\bar{P}_1 = \frac{\gamma}{\bar{h}_1}(1+\Theta) - \frac{1}{\bar{h}_1^2}\Pi(1-\bar{x})^2 \quad (35)$$

The profile of Eq. (34) together with the accompanying static pressure are shown in Fig. 5. The static pressure rises and falls along the co-ordinate x while the height of the manifold increases continuously.

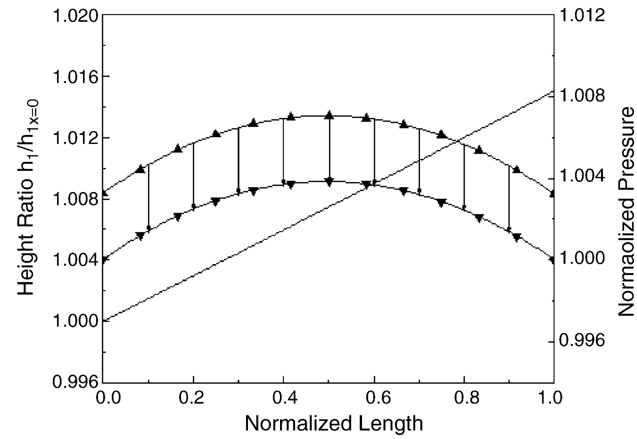

Fig. 5. Profile of manifold shape for $h_1(x)=h_2(L-x)$ and normalized static pressure at upper manifold (Z-type).

3.2. U-type

For a U-type manifold, Eq. (23) is substituted for $\tilde{q}$ in Eq. (20) to produce:

$$\frac{M_1}{h_1} - \frac{M_2}{h_2} - \rho q^2(1-\bar{x})^2\left(\frac{1}{h_1^2} - \frac{1}{h_2^2}\right) = \Omega \quad (36)$$

Rearranging terms after the substitution of Eqs. (21) and (22) for M_1 and M_2 yields the second order manifold equation for U-type. This equation appears to be very complicated but, at most, is second order for either h_1 or h_2.

$$\frac{h_{1,\bar{x}=0}}{h_1}\left(\rho\frac{q^2}{h_{1,\bar{x}=0}^2} + P_{\text{amb}} + \Omega\right) - \frac{h_{2,\bar{x}=0}}{h_2}\left(\rho\frac{q^2}{h_{2,\bar{x}=0}^2} + P_{\text{amb}}\right) - \rho q^2(1-\bar{x})^2\left(\frac{1}{h_1^2} - \frac{1}{h_2^2}\right) = \Omega \quad (37)$$

From the definition of M_1, the static pressure at the upper manifold is:

$$P_1 = \frac{h_{1,x=0}}{h_1}(P_{\text{amb}} + \Omega) + \frac{\rho q^2}{h_1^2}\left(\frac{h_1}{h_{1,x=0}} - (1-\bar{x})^2\right) \quad (38)$$

3.2.1. $h_1(x) = const$

The first case to be explored for the U-type configuration is the upper manifold with a uniform cross-section. The cross-section of the lower manifold is changed so that there is an even distribution among the channels. During the derivation, scaling variables α, Π and Θ are defined as in the previous section for Z-type configuration with $h_{2,\bar{x}=1}$ replaced by $h_{2,\bar{x}=0}$, i.e.:

$$h_{2,\bar{x}=0} = \alpha h_1, \qquad \frac{\rho q^2}{P_{\text{amb}} h_{2,\bar{x}=0}^2} \equiv \Pi,$$

$$\frac{\Omega}{P_{\text{amb}}} \equiv \Theta, \qquad \frac{h_2}{h_{2,\bar{x}=0}} \equiv \bar{h}_2,$$

$$[1 + \alpha^2\Pi(2\bar{x} - \bar{x}^2)]\bar{h}_2^2 - (\Pi+1)\bar{h}_2 + \Pi(1-\bar{x})^2 = 0 \quad (39)$$

The profiles of the lower manifold for changes in the parameter α from 0.5 to 2.0 are given in Fig. 6. For $\alpha = 1.0$, the lower manifold with a uniform cross-section gives rise to an even distribution among the channels. Though this is the result obtained by neglecting the friction at the wall, it still reports that the U-type is more efficient than Z-type configuration in producing an even distribution. Unlike the Z-type, a lower manifold of the U-type is required to have an increasing or decreasing cross-section

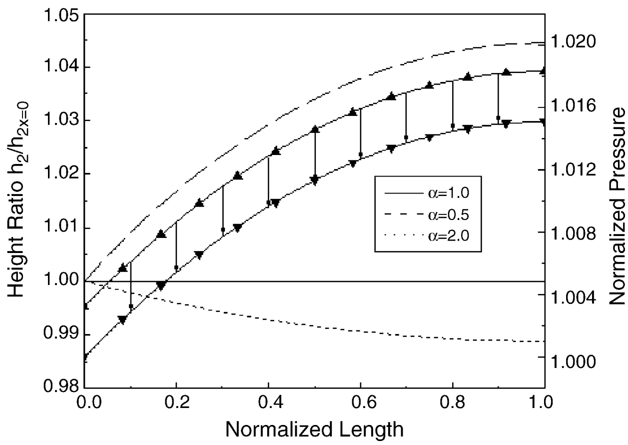

Fig. 6. Profile of lower manifold for $h_1(x)$ = const and normalized static pressure at upper manifold (U-type).

in the direction of x depending on its size, i.e.:

$$\bar{P}_1 = 1 + \Theta + \alpha^2 \Pi (2\bar{x} - \bar{x}^2) \quad (40)$$

The static pressure increases continuously along the co-ordinate x regardless of the manifold shape. The Z-type manifold could have an increasing or decreasing profile of static pressure depending on its size and design. By contrast, the static pressure of the U-type manifold is not sensitive to the manifold shape but is changed by the loss or the gain of the inertia.

3.2.2. $h_2(x)$ = const

The next case of constant h_2 also suggests scaling variables β, Π and Θ. The physical meaning of each variable is the same as that discussed above for the Z-type manifold (see Section 3.1.1), i.e.:

$$h_{1,\bar{x}=0} = \frac{h_2}{\beta}, \qquad \frac{\rho q^2}{P_{\mathrm{amb}} h_2^2} \equiv \Pi,$$

$$\frac{\Omega}{P_{\mathrm{amb}}} \equiv \Theta, \qquad \frac{h_1}{h_{1,\bar{x}=0}} \equiv \bar{h}_1,$$

$$(1 + \Theta + \Pi(2\bar{x} - \bar{x}^2))\bar{h}_1^2 - (1 + \Theta + \beta^2 \Pi)\bar{h}_1 + \beta^2 \Pi (1 - \bar{x})^2 = 0 \quad (41)$$

This case produces the same profile for the manifold shape as that shown in Fig. 6 if α is replaced by $1/\beta$, which is expected from the symmetry:

$$\bar{P}_1 = \frac{1}{\bar{h}_1}(1 + \Theta + \beta^2 \Pi) - \frac{1}{\bar{h}_1^2}\beta^2 \Pi (1 - \bar{x})^2 = 1 + \Theta + \Pi(2\bar{x} - \bar{x}^2) \quad (42)$$

3.2.3. $h_1(x) = h_2(x)$

The relationship $h_1(x) = h_2(x) =$ const is the only solution to satisfy the condition $h_1(x) = h_2(x)$. The situation where of $\alpha = 1.0$ in Section 3.2.1 corresponds to this case as shown by the data in Fig. 6, i.e.:

$$\bar{P}_1 = 1 + \Theta + \Pi(2\bar{x} - \bar{x}^2) \quad (43)$$

4. Conclusions

A method has been developed for designing fuel-cell manifolds to distribute the reactants among the channels within bipolar plates. Expressions for the manifold height have been derived for Z-type and U-type configurations after neglecting the friction term. Criteria for determining the validity of the current model are also proposed. Some cases are explored to find the specific design that satisfies the derived manifold equation for each configuration. The static pressure within each manifold is calculated and can be used to estimate the pressure requirement at the inlet to drive the specific flow rate. During such derivation, scaling variables are defined and are based on the operating conditions as well as on the geometric configurations of the channel and the manifold.

Reference

[1] S. Maharudrayya, S. Jayanti, A.P. Deshpande, J. Power Sources 144 (2005) 94–106.